International Journal of Medical Toxicology & Legal Medicine Volume 27, No. 4S, 2024
e-ISSN: 0974-4614
p-ISSN: 0972-0448
https://doi.org/10.47059/ijmtlm/V27I4S/115

Chlorella Vulgaris has a Protective Effect against Gibberellic Acid-induced Lung Injury in Male Albino Rats

Rasha A. Alshali [1*]

[1]Department of Clinical Anatomy, Faculty of Medicine, King Abdulaziz University, Jeddah, KSA,
Email: r.alshali@yahoo.com
*Corresponding Author

Received: 18.09.2024 Revised: 12.10.2024 Accepted: 22.11.2024

ABSTRACT

Background: Gibberellic acid (GA3) is a plant growth regulator used extensively in many nations that affects health of humans and animals. This study assessted the potential harm of GA3 on the lung and investigated the potential protection of Chlorella vulgaris (ChV) against the GA3-induced structural and morphometric alterations in the lung.

Materials & methods: Twenty-four adult male albino rats were divided into: negative control group (G1), ChV-group (G2) treated with ChV (300mg/kg body weight once daily for 14 days), GA3-treated group (G3) treated with GA3 (55mg/Kg once daily for 14 days), and GA3/ChV-treated group (G4) concomitantly treated with ChV and GA3 with the same dose and duration. Lung specimens were processed for microscopic assessment, biochemical study, morphometric analysis, and an immunohistochemical study.

Results: Thickened interalveolar septum with inflammatory cellular infiltration and congested thick wall blood vessels were observed in the GA3-treated group. A statistically significant increase in the area percent of collagen fibers, the mean thickness of the interalveolar septa, and a significant decrease in the mean alveolar space surface area were detected in the GA3-treated group compared to the negative control group. Immunohistochemical study showed a strong positive cytoplasmic reaction of Caspase-3 in GA3-treated group. A significant increase in TNF-α was detected in GA3-treated group compared to the negative control group. In contrast, obvious improvement of these findings was observed in rats treated with both ChV and GA3.

Conclusion: The histological, morphometrical, and biochemical alterations brought on by Gibberellic acid in the lung could be ameliorated by Chlorella vulgaris.

Keywords: Gibberellic acid, Chlorella vulgaris, Lung injury, rat, histological, TNF-α

1. INTRODUCTION

Chemicals have been used extensively in agriculture and livestock in recent years such as plant growth regulators (PGRs) that are applied to enhance crop development. The most well-known of these substances is phytohormones, which are PGRs also known as plant hormones [1]. They consist of cytokinin, gibberellins, auxins, nitric oxide, and abscisic acid. Gibberellins are also among the most significant phytohormones that promote plant growth by breaking down the DELLA protein, a negative growth regulator [2]. Gibberellic acid (GA3), is a member of the gibberellin family and one of the most significant growth-stimulating plant hormones has been utilized extensively in many nations to encourage the elongation, division, and growth of numerous plant species [3,4]. Scientists are extremely concerned about GA3's startling toxicity and detrimental impacts on human and animal health because it can linger in the soil for several months. Furthermore, the Environmental Protection Agency has concluded that using it is only permitted at very low doses [5–7]. GA3 was identified by the World Health Organization (WHO) as a pesticide-related plant growth regulator [8]. GA3 may pose a concern to anyone who is professionally exposed as well as consumers in general if they eat contaminated food. Residue exposure might also occur by drinking water [9–11]. These substances irritate the skin, mucous membranes and eyes. Due to its easy absorption through the skin, the mouth, or inhalation, it can cause damage to the liver, kidney, lung, muscle, and brain tissues [12,13]. Despite GA3's widespread use in agriculture, very few studies have looked at any potentially harmful effects it

may have on people and animals. Thus, this topic has recently piqued the curiosity of numerous scholars. The single-celled green algae *Chlorella vulgaris* (ChV) is distinguished by its great production and ease of growing. It also contains exceptional amounts of protein, lutein, chlorophyll, and many other essential micronutrients [14,15]. Asia is where ChV was initially produced and consumed, mostly in Japan [16]. These days, ChV is manufactured in several nations, such as China, the US, Taiwan, and Indonesia, and it is exported and sold abroad as a dietary supplement and functional food [17]. The Food and Drug Administration (FDA) lists *C. vulgaris* as a safe algae [18]. With 60% protein, 20 vitamins, 18 amino acids, and minerals including iron, potassium, calcium, phosphorus, and magnesium, it is regarded as a superfood [19]. Previous research in animals has shown that ChV supplements can decrease blood sugar and cholesterol levels, and have immune-modulating and antioxidant effects [17]. ChV has been shown in several human trials to lower oxidative stress, and inflammation, enhance lipid profiles, and lower blood sugar levels [20–22], while not all the studies have shown this [23]. Thus, the current study aims to assess the potential harm of GA3 on the lung of adult male albino rat and investigate any potential defense mechanism provided by *Chlorella vulgaris* (ChV) against the structural and morphometric alterations in the lung caused on by GA3 administration.

1. Material and methods:

1.1. Ethical considerations

The experimental protocols had been approved by the Institutional Animal Care and Use Committee, Kind Abdulaziz University, Jeddah, Saudi Arabia. All animal procedures were conducted rapidly and carefully to reduce pain and stress-related changes. The procedures were carried out by the ethical standards set forth by the National Institutional Animal Care and Use Committee and the Committee for the Control and Supervision of Experiments on Animals.

1.2. Chemicals

The gibberellic acid (2,4a,7-Trihydroxy-1-methyl-8-methylenegibb-3-ene1,10-dicarboxylic acid 1,4a-lactone, 99% purity) was obtained from Sigma-Aldrich (Saint Louis, MO, USA) as a white crystalline powder, it was dissolved with distilled water. The chlorella vulgaris powder was supplied by Algal Biotechnology Unit (National Research Centre, Dokki, Giza, Egypt). The dried extract was refrigerated and redissolved in regular saline (0.9%) just before oral administration. Tumor necrosis factor-alpha (TNF-α) ELISA kits were acquired from Abcam's Co. (catalog No. ab 100785).

1.3. Animals and Experimental Design

In the current study, twenty-four adult male Albino Wister rats weighing between 200 and 250 grams were used. The rats were acquired from the Faculty of Pharmacy, King Abdulaziz University in Jeddah, Saudi Arabia. All animals were housed in groups in plastic cages at 21−22 °C, 55−60% humidity, and a 12 h light:12 h dark cycle (lights on at 07:00 AM). They were fed commercial rat pellets and given access to drinking water after being acclimated to their surroundings before the experiment. The Committee for Control and Supervision of Animal Studies' recommendations for the use and care of experimental animals, as well as national institutional requirements for animal care, were followed in the execution of all experimental procedures. The rats were divided randomly into four groups, each with six rats.

Negative Control group (G1): in this group rats were not given any treatment.

ChV-treated group (G2): The rats in this group were given 300 mg/kg body weight, which was diluted with 1 ml of distilled water and given orally every day for 14 days using a 27-gauge stainless steel feeding needle [24].

GA3-treated group (G3): For 14 days, the rats were given GA3 orally via gavage at a dose of 55 mg/kg body weight (dissolved in distilled water) [25].

GA3/ChV-treated group (G4): For 14 days, the rats were given GA3 at a dose of 55 mg/kg body weight and ChV at a dose of 300 mg/kg body weight once a day. At the end of the experiment, the rats were anesthetized with sodium pentobarbital (100 mg/kg) and sacrificed [26]. The heart was perfused by saline solution through the left ventricle until the coming out fluid, from the right atrium after being opened, was blood-free, then perfusion with 10% formalin was performed. To collect lung tissues for histological and biochemical analysis, a ventral midline incision, exposure, dissection, and immediate excision were performed. The left lung of each animal was divided into 2 equal parts. The first part was used for lung homogenate preparation. The second part was used to prepare paraffin blocks for histopathological and immunohistochemical examination. All ethically approved procedures for handling, housing, and care of the rats were carried out in firm accordance with the International Guidelines for the Care and Use of Laboratory Animals.

1.4. Histological Examination

1.4.1. Paraffin block preparation

Lung tissue specimens from the lower third of the left lung were processed to prepare paraffin sections 5µm thickness. To sum up, the samples were fixed in 10% buffered formalin, dehydrated in ethyl alcohol at progressively higher concentrations (70%–100%), and then embedded in paraffin. The histological details were identified using hematoxylins and eosin (H&E) [27], and the collagen fibers were demonstrated using Masson's trichrome stain [28]. Stained slides were evaluated and photographed on camera with an optical microscope (Leica DM500) and a digital camera (Leica ICC50 W Camera Modul) for histopathological and morphometric assessments.

1.4.2. Immunohistochemical

The avidin-biotin-peroxidase method was used to stain the sections for immunohistochemical staining to localize Caspase-3 [7,29]. To reveal antigens, paraffin sections with a thickness of 5 µm were deparaffinized and exposed to 0.01 M citrate buffer for 10 minutes. Subsequently, the sections were incubated for a whole night at 4°C in a humid chamber using a diluted rabbit monoclonal Caspase-3 antibody (SAB5700914, Sigma Aldrich, Cairo, Egypt) as the primary antibody. The procedures were to wash in PBS buffer and incubate with biotinylated secondary antibody for one hour at room temperature. Streptavidin peroxidase was then added for 10 min and rinsed again three times in PBS. Immunoreactivity was visualized using 3,3′-diaminobenzidine-hydrogen peroxide as a chromogen. Sections were counterstained with Mayer's hematoxylin. The negative control sections were prepared by excluding the primary antibodies.

1.5. Tissue homogenate:

Lung homogenates were prepared using a previously mentioned technique [16]. TNF-α was quantified in lung homogenates using an ELISA kit (bought from Abcam's Co.; catalog number: ab208348), using the appropriate antibodies and the manufacturer's instructions. Using Hitachi spectrophotometry (Tokyo, Japan), the optical density (OD) was determined spectrophotometrically at 450 nm.

1.6. Morphometric analysis:

Image J was used to analyze the images. The mean thickness of the interalveolar septum (µm) of the hematoxylin and eosin-stained sections, the mean alveolar space surface area in (μm^2) of H&E-stained sections, and the mean area % of collagenous fibers of the Masson's trichrome stained sections were quantified from 10 randomly selected images for each group at a magnification of X400 [30].

1.7. Statistical Analysis:

Statistical analysis was done using the Statistical Package Social Sciences (SPSS) version 23 for windows® (IBM SPSS Inc., Chicago, Illinois, USA). Statistical analysis was accomplished using the ANOVA (one-way analysis of variance test) test followed by the post hoc Tukey test. Data were represented as mean ± SD. P-value < 0.05 was considered of statistical significance. All the graphs were performed using GraphPad Prism software version 10.1.2 for Mac (GraphPad Software, San Diego, CA, USA).

2. Results:

2.1. Light microscopic examination:

2.1.1. Haematoxylin and eosin stain:

H&E-stained sections from specimens in the negative control group (G1) showed the typical architecture of the lung. The segments included blood vessels, bronchioles, lung alveoli, and alveolar sacs divided by thin interalveolar septa. Various-sized bronchioles with spirally structured smooth muscle layer, adventitia of areolar connective tissue, and intact folded mucosa covered with simple columnar ciliated epithelium all. There were normal-thickness blood vessels visible. Pneumocytes Type I, which are flat cells with flattened nuclei, dominated the alveolar spaces, whereas Pneumocyte Type II, which are cuboidal cells with rounded nuclei, were most observed at the angles **(Figure 1A-C)**.

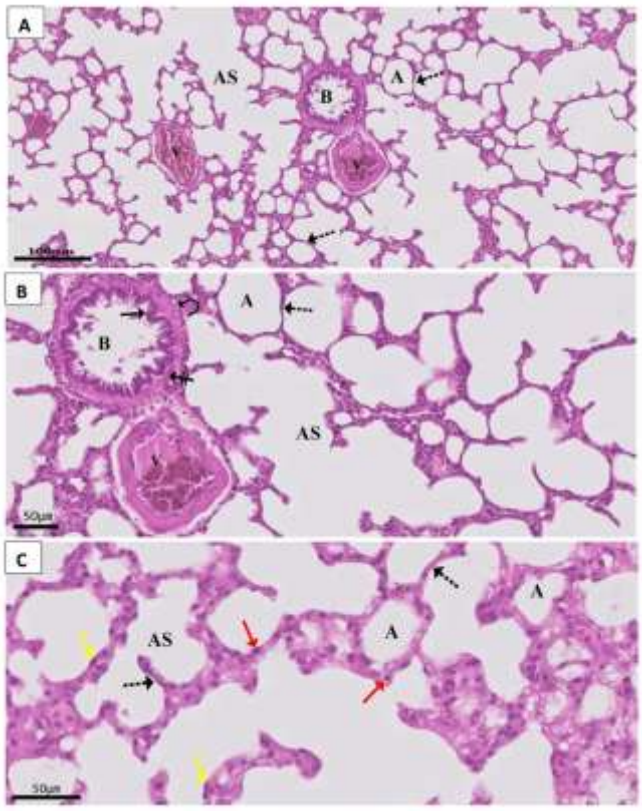

Figure 1: Photomicrograph of a section in rat lung of the Negative control group (G1) showing: (A) normal lung architecture with a clear alveolar sac (AS), alveoli (A), and bronchiole (B). **(B &C)** thin interalveolar septa (dot arrow), blood vessels (V), and bronchiole (B) with folded mucosal lined by simple columnar partially ciliated epithelium (↑) with continuous thin smooth muscle layer (double stroke↑) and a thin layer of connective tissue (curved arrow). Thin interalveolar septum (dot arrow) with flattened type-I pneumocyte (yellow ↑) and cuboidal type-II pneumocyte with rounded nuclei (red ↑) lining the alveolar space (A) is seen.

H&E A X10, B X20 & C X40

The group receiving ChV treatment (G2) showed intact lung histological structure, resembling the negative control group with normal bronchioles, blood vessels, alveoli, alveolar sacs, and interalveolar septa architecture **(Figure 2A-C)**.

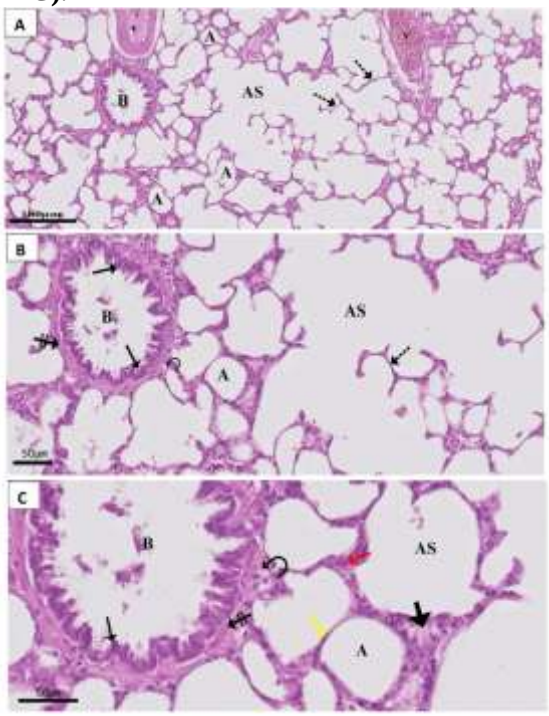

Figure 2: Photomicrograph of a section in rat lung of ChV-group (G2) showing:
(A-C) the normal lung construction; expanded alveoli (A) and alveolar spaces (AS) separated by thin

interalveolar septa (dot arrow), bronchioles (B), and blood vessels (V). The bronchioles (B) appear lined by simple columnar partially ciliated epithelium (↑), a thin smooth muscle layer (double stroke↑), and a thin layer of connective tissue (curved arrow). Expanded alveoli (A) separated by thin interalveolar septa (dot arrow) are seen. The alveoli (A) are lined by pneumocytes type I (yellow ↑), pneumocytes type II (red ↑), and with normal pulmonary capillaries (arrowhead).

H&E A X10, B X20 & C X40

The GA3-treated group's (G3) lung sections revealed a distorted lung architecture, with clearly visible thicker interalveolar septa, reduced alveolar spaces, or even collapsed alveolar spaces, offset by dilated adjacent alveoli. There was also a noticeable diffuse infiltration of mononuclear cells in the peribronchiolar. There was a significant deposition of hemosiderin granules. Most of the blood vessels in the lungs were thickened, dilated, and congested. The bronchioles showed intrabronchial cellular debris and an unorganized wall with the epithelium detached from its basement membrane. Numerous fibroblasts were noticed in the interstitial tissue and surrounding the bronchioles. Notice that there was eosinophilic excaudate in the lung interstitium **(Figure 3A-D)**.

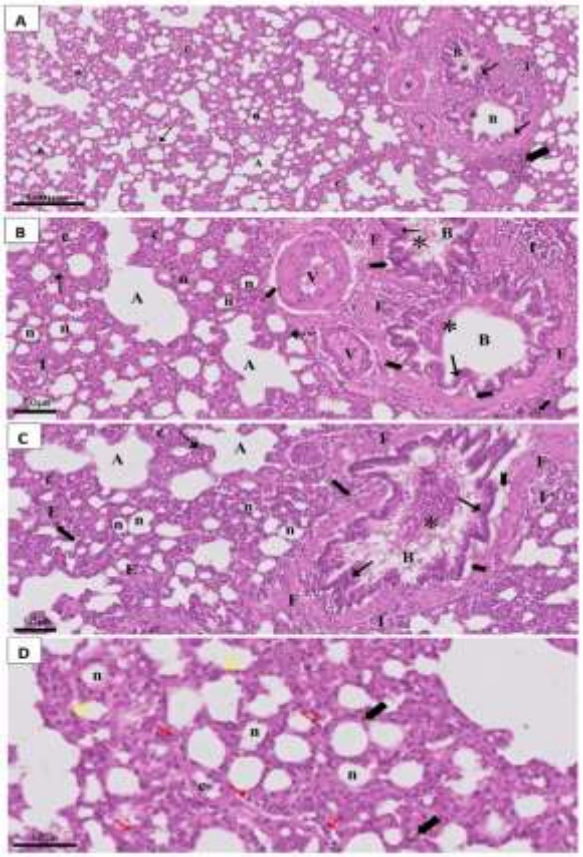

Figure 3: Photomicrograph of a section in rat lung of GA3-treated group showing:
(A-C) a disturbed lung architecture with obvious markedly thickened interalveolar septa (dot arrow) with narrowing (n) of alveolar spaces or even collapse (c) of alveolar spaces with compensatory expansion of adjacent alveoli (A). A marked diffuse peribronchial mononuclear cellular infiltration (I) is also seen. Hemosiderin granules (thick arrow) deposition is noticed. The pulmonary blood vessels (V) are dilated, thickened, and congested. The bronchioles (B) show a disorganized wall (↑) and separated epithelium from its basement membrane (bifid arrow) and the presence of intrabronchial cellular debris (*). Numerous fibroblasts (F) are noticed in the interstitial tissue and around the bronchioles. Notice eosinophilic excaudate (E) is seen. **(D)** Notice most of the type-I pneumocytes (yellow ↑) with pyknotic nuclei and type-II pneumocytes (red ↑) with vacuolated cytoplasm and pyknotic nuclei are seen.

H&E A X10, B X20 & C X40

Following 14 days of oral Chlorella vulgaris GA3/ChV treatment, the majority of bronchioles, alveoli, and interalveolar septa returned to their typical morphology. Nonetheless, a small number of regions displayed some alveolar narrowing and collapsing, along with moderate interstitium cellular infiltrations **(Figure 4A-C)**.

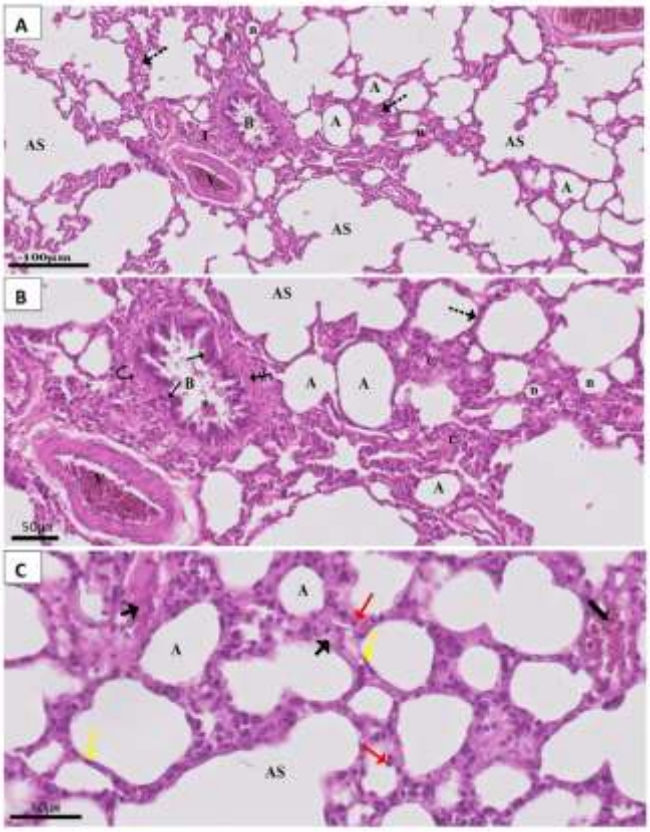

Figure 4: Photomicrograph of a section in rat lung of GA3/ChV-treated group showing:
(A& B) Normal bronchiolar epithelium with restored mucosal folding (↑) and continuous circularly arranged smooth muscle layer (double stroke↑) with a thin layer of connective tissue (curved arrow) is seen. Clear alveolar sacs (AS), alveoli (A), and relatively thin interalveolar septa (dot arrow). A bronchiole (B) with folded mucosal lining and continuous muscle layer (double stroke↑), blood vessel (V) with a thick wall and intact intima, residual interstitial cellular infiltration (I) near the bronchiole. Notice few areas of collapse and narrow alveoli are seen. **(C)** Expanded alveoli (A) separated by thin interalveolar septa (dot arrow) are seen. Type-I (yellow↑) and type-II pneumocytes (red ↑) with normal pulmonary capillaries (arrowhead) are nearly similar to the control group.

H&E A X10, B X20 & C X40

2.1.2. Masson's trichrome stain:

Masson's trichrome-stained sections of the **negative control group (G1) and ChV-treated group (G2)** revealed fine collagen fibers in the interalveolar septa, the adventitia of bronchioles and adventitia of the blood vessels **(Figures 5A& B)**. The **GA3-treated group** showed obvious deposition of collagen fibers in the thickened interalveolar septa as well as in the adventitia of bronchioles and blood vessels **(Figure 5C&D)**. **GA3/ChV-treated group (G4)** revealed deposition of scattered fine collagen fibers in the thickened interalveolar septa, adventitia of bronchioles, and blood vessels **(Figure 5E)**.

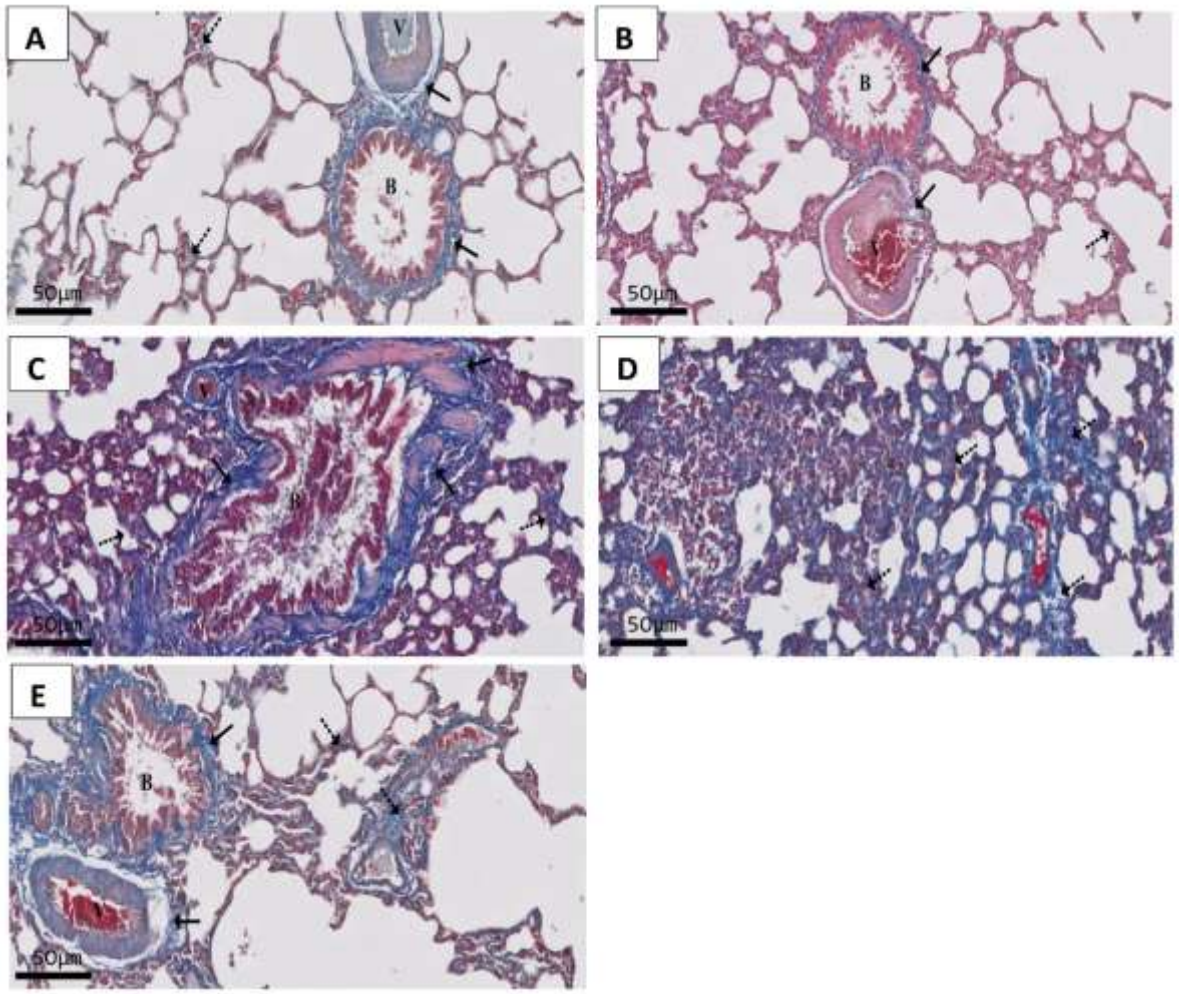

Figure 5: Photomicrograph of a section in rat lung of
(A) Negative control group (G1) and (B) ChV-group (G2) showing fine collagen fiber (↑) scattering in the walls of a respiratory bronchiole (B), around the blood vessels (v), and in the interalveolar septa (dot arrow). **(C) & (D) GA3-treated group** showing massive deposition of collagen fibers (↑) in the wall of a bronchiole (B)and surrounding blood vessels (V). Collagen fibers in the thickened interalveolar septa (dot arrow) are also detected. **(E) GA3/ChV-treated group** showing moderate scattered collagen fibers (↑) in the interalveolar septa (dot arrow), adventitia of the bronchioles (B), and that of the blood vessels (V).

Masson Trichrome stain X20

2.2. Immunohistochemistry (IHC) for the detection of Caspase-3:

Caspases-3 positive immunohistochemical staining is shown by brown cytoplasmic staining, which serves as an indicator of the degree of nuclear apoptosis. Negative cytoplasmic staining of caspase-3 was found in the cytoplasm of bronchioles cells, alveolar, and interalveolar septal and along the endothelial lining of blood vessels of the negative control group (G1) and in the ChV treated group (G2). Notice, that there were a few moderate positive nuclear browning reactions of the cells interspersed in the interstitium of the lung inside the area of aggregation of negative nuclear reactions were seen **(Figure 6A &B)**.

The majority of the cells in the GA3-treated group (G3) filled the bronchiole lumen and displayed a huge, robust positive brownish cytoplasmic reaction. In the lung's interstitium, there was a noticeable mass of positive brownish cytoplasmic reaction cells, which were most likely apoptotic alveolar epithelial cells **(Figure 6C)**. Conversely, a large area of negative brownish nuclear reaction aggregation was likely caused by the aggregation of mononuclear inflammatory cells in the lung's interstitium **(Figure 6D)**.

It's interesting to note that it was only weakly expressed in the cytoplasm of the alveolar, bronchioles, lung interstitium, septal, and endothelial lining of some blood vessels in the GA3/ChV-treated group (G4). The majority of the cells in the bronchiole lining and alveolar epithelial cells displayed a negative nuclear brownish response. In the lung's interstitium, a moderately strong positive nuclear brownish response was observed **(Figure 6E)**.

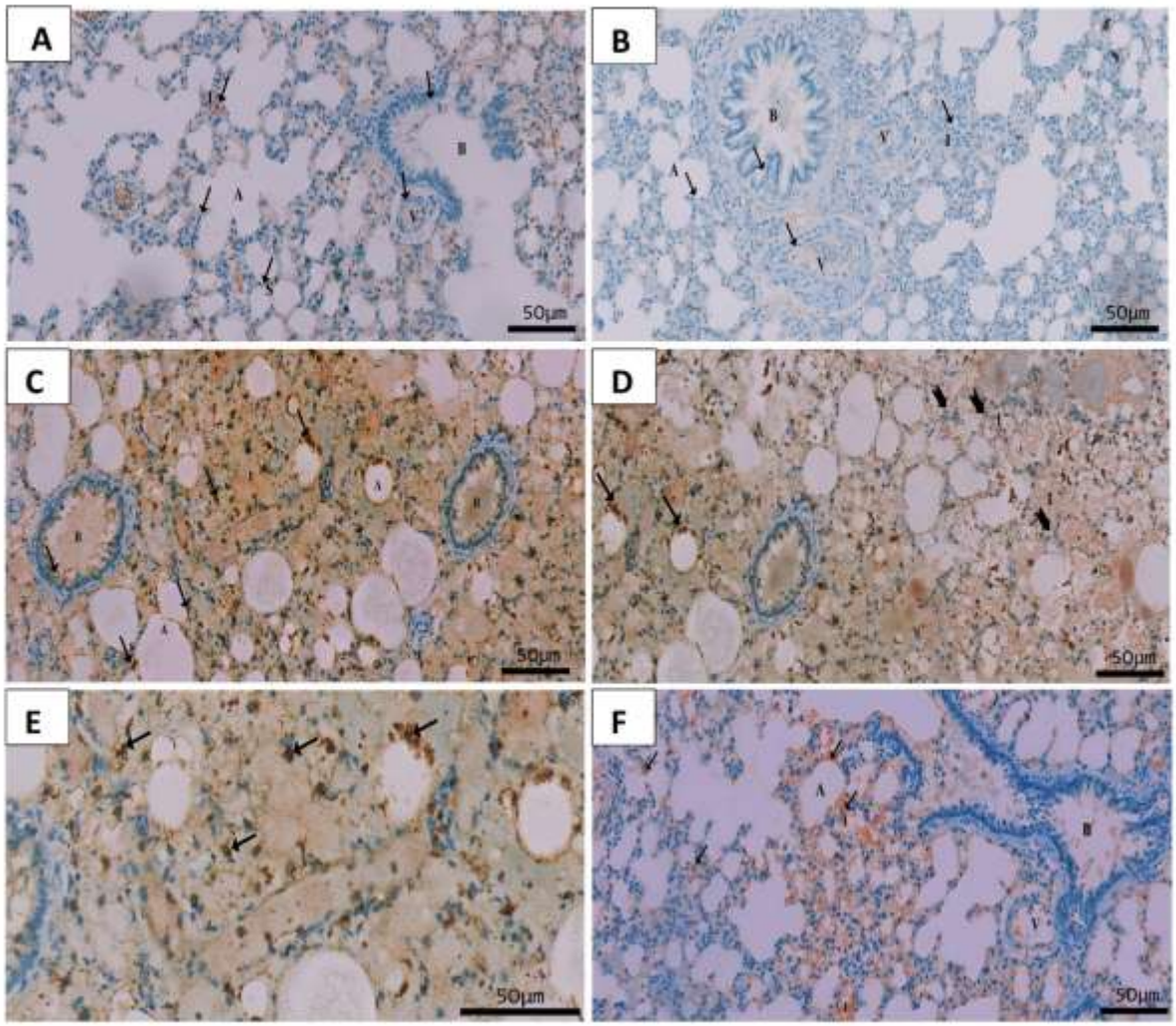

Figure 6: Photomicrograph of a section in rat lung of
((A) Negative control group (G1) and (B) ChV-group (G2) most of the cells reveal negative nuclear brownish reaction (↑) in most of the cytoplasm of bronchial cells (B), alveolar cells (A), interalveolar septal cells (S) and along the endothelial lining of blood vessels (V). Notice, that there are a few mild positive nuclear browning reactions of the cells interspersed in the interstitium (I) of the lung inside the area of aggregation of negative nuclear reactions are seen.
(C-E) GA3-treated group showing massive strong positive brownish caspase-3 expression (↑) in the cytoplasm of bronchial cells (B), alveolar cells (A), and interalveolar septal cells (S). Notice the area of massive (↑) aggregation of positive brownish nuclear reaction and the area of negative cytoplasmic reaction (bifid arrow) in the interstitium (I) of the lung.
(F) GA3/ChV-treated group showing moderate brownish caspase-3 expression (↑) in the cytoplasm of bronchial cells (B), alveolar cells (A), septal cells (S) and along the endothelial lining of some blood vessels (V). Notice, that few moderate positive nuclear brownish reactions in the interstitium (I) of the lung are seen.

Immunostaining caspase-3 A- D,&Fx 20, Ex40

2.3. Morphometric and statistical results:

As shown in **Figure (7A)**, the mean area percentage of collagen fibers was 4.80±0.45 in the negative control group (G1). The negative control group exhibited a significant (P<0.0001) decrease in the mean area percentage of collagen fibers as compared to both the GA3-treated group (35.57±0.84) and GA3/ChV-treated group (8.49±0.90). However, there was a non-significant difference between G1, and rats that received ChV alone (P>0.99). Meanwhile, G4 (GA3/ChV-treated group) showed a significant decrease in the mean area percentage of collagen fibers as compared to G1 (4.80±0.45) and G2 (4.80±0.62), respectively.
As shown in **Figure (7B)**, the mean thickness of the interalveolar septa was 4.86± 0.97µm in the negative control group (G1). The negative control group exhibited a significant (P<0.0001) decrease in the mean thickness of the interalveolar septa as compared to both the GA3-treated group (44.44±2.63

µm) and GA3/ChV-treated group (15.87±3.31 µm). However, there was a non-significant difference between G1, and rats that received ChV alone (P >0.99). Meanwhile, G4 (GA3/ChV-treated group) showed a significant (P<0.0001) decrease in the mean thickness of the interalveolar septa as compared to G1 (4.86± 0.97±1.29 µm) and G2 (4.70± 0.74µm), respectively.

As shown in **Figure (7C)**, the mean alveolar space surface area was 775.3±42.71 μm^2 in the negative control group (G1). The negative control group exhibited a significant (P<0.0001) increase in the mean alveolar space surface area as compared to both the GA3-treated group (209.6±32.50 μm^2) and GA3/ChV-treated group (586.9±71.00 μm^2). However, there was a non-significant difference between G1, and rats received ChV alone (P=0.73). Meanwhile, G4 (GA3/ChV-treated group) showed a significant decrease of the mean alveolar space surface area as compared to G1 (775.3±42.71μm^2) and G2 (816.2±57.23μm^2), respectively.

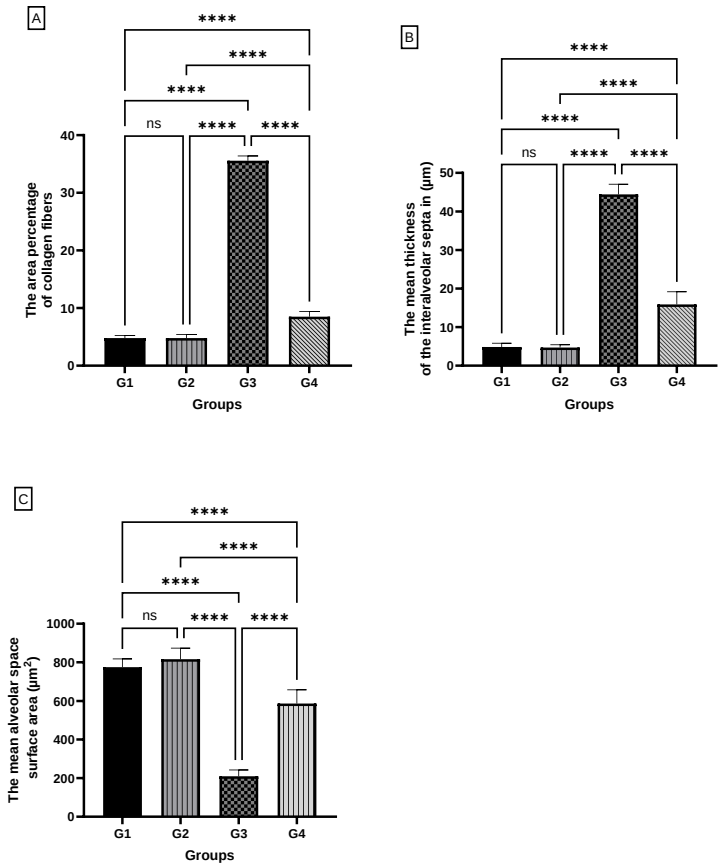

Figure 7: Protective effect of *Chlorella vulgaris* (ChV, 300 mg/kg/BW) against GA3 (55 mg/kg/BW)-induced changes on (A):

The mean area percentage of collagen fibers, (B) the mean thickness of the interalveolar septa (µm), and (C) the mean alveolar space surface area (μm^2) in lung tissue of rats in different experimental group. Values are means ± standard deviation (SD) for 6 different rats/groups. ns: non-significant and ****significant at P <0.0001. G1: Negative Control group, G2: ChV- group, G3: GA3-treated group, and G4: GA3/ChV-treated group

2.4. Biochemical results:

As compared with G1, there was a significant (P<0.0001) increase in TNF-α concentration in G3 (35.36 ± 1.26 pg/ml). Animals in G3 showed a significant (P<0.0001) increase in TNF-α concentration as compared to G4 (12.40 ± 1.84 pg/ml). Meanwhile, G4 showed a significant (P<0.0001) decrease in TNF-α concentration as compared to G1 (8.88± 1.26 pg/ml) and G2 (9.06± 0.9331 pg/ml), respectively **(Figure 8)**.

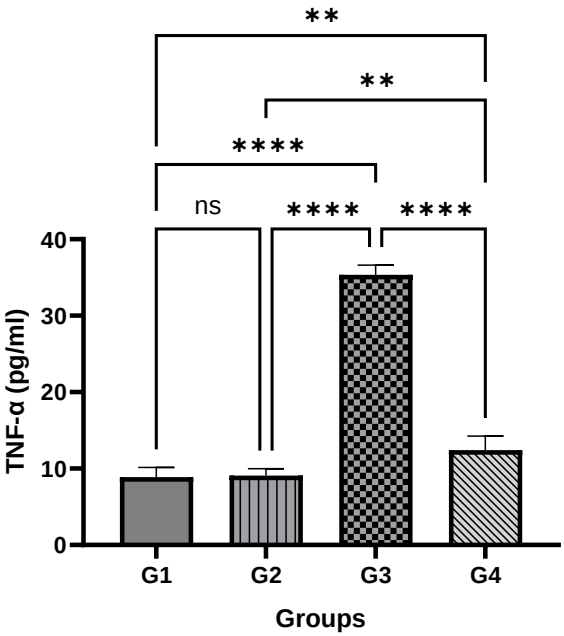

Figure 8: Protective effect of *Chlorella vulgaris* (ChV, 300 mg/kg/BW) against GA3 (55 mg/kg/BW)-induced changes on the expression of TNF-α pg/ml in lung tissue homogenate of rats in different experimental group.

Values are means ± standard deviation (SD) for 6 different rats/groups. ns: non-significant, **significant at P < 0.01, and **** significant at P <0.0001. G1: Negative Control group, G2: ChV- group, G3: GA3-treated group, and G4: GA3/ChV-treated group

3. Discussion:

Recently, there has been a lot of interest in the study due to the extensive usage of plant growth hormones in agriculture and the potential effects on human health. One of the PGRs, GA3, is harmful to the lungs and other soft organs [24]. Despite the concerning toxicity that GA3 has brought to the mammalian system, it is nevertheless widely used in many nations [31]. Its potentially dangerous effects on mammals have not been thoroughly investigated, particularly concerning the in-depth structural effects on the lung. Chlorella is a type of green alga that contains one cell and is used more often than other natural items. Consequently, we shed insight on Chlorella vulgaris's ability to shield the lungs from GA3's detrimental effects in this study. The present study's histological analysis of H&E-stained sections from the GA3 group (G3) revealed severe alveolar damage, including thickened interalveolar septa and blood vessel walls with narrowing or even collapse of the intervening alveoli (atelectasis), along with loss of normal lung architecture. Other alveoli appeared enlarged (dilated). Similar findings were recorded by Dong et al. [32], Zakaria et al. [30], and Bassiouny et al. [33]. They created an idiopathic pulmonary fibrosis experimental model. They used bleomycin and reported the same results. They clarified that this might be because profibrotic and inflammatory cytokines like interleukin-1 and macrophage inflammatory protein-1 are produced by alveolar macrophages in response to stimulation. Furthermore, these cytokines induce type II pneumocyte hyperplasia, which in turn causes fibroblast activation and additional proliferation, increasing collagen deposition and ultimately alveolar collapse. Additionally, a few of these cytokines function as chemoattractant, which promotes the recruitment of inflammatory cells and cellular infiltration [30,32,33]. This was consistent with the current study, which also found extensive cellular infiltration around blood vessels, in the peribronchiolar space, and within the inter-alveolar septa. This is consistent with the findings of Alsemeh et al., who noted cellular infiltration in the rat livers after GA3 treatment [34]. Desai et al. found a correlation between the early stages of pulmonary fibrosis and inflammatory responses, such as an influx of neutrophils, lymphocytes, and macrophages [35]. Ornatowski et al. clarified that the oxidative stress linked to this inflammatory cellular infiltration produced mediators like interleukin 8 and cytokine-induced neutrophil chemoattractant, which draw inflammatory cells into the microcirculation and eventually to the lung interstitium because free radicals damage endothelial cells [36]. The present study's observation of alveolar collapse was explained by several authors [37–39]. They noticed that inflammation-induced inability of the alveoli to expand [39] or surfactant malfunction due to shape deformity and reduction in lamellar body number [37,38]. However, the

current study's observation of some alveoli's overexpansion is consistent with the findings of Knudsen et al., who discovered that in a bleomycin rat model, increasing lung damage, alveolar collapse, and increased dilation of patent (open) alveoli [40]. The present study's morphometrical and statistical analysis validated the histology outcome. Furthermore, the GA3-treated rat lung's respiratory bronchioles had cellular debris in their lumina and many cells that had exfoliated from their lining epithelium. It was discovered that the lining epithelium in this investigation was disordered and appeared to have separated from its foundation membrane. This can be explained by the toxicity of GA3 on the bronchiole mucosal lining. El Bana and Shawky noticed comparable findings in the lungs of rats given amiodarone. They stated that the most typical manifestation of amiodarone-induced lung illness is interstitial pneumonitis and pulmonary toxicity [41].Furthermore, we observed thickening and congestion in the pulmonary interstitium blood vessel walls with homogenous eosinophilic material. The kidneys and livers of rats given gibberellic acid showed signs of degeneration, cellular infiltration, congestion, and hemorrhage [34,42,43]. Pulmonary hypertension may arise as a result of pulmonary arteriole wall thickening [44]. Furthermore, the current study's findings were consistent with those of Kamel et al., who in their investigation of rats receiving methotrexate medication interpreted the development of eosinophilic material and cellular aggregates of fibroblasts and macrophages as plasma exudates created by alveolar injury [45].Haemosiderin granules were seen in the interalveolar septa of the lung sections treated with GA3 in the current study. This was consistent with the histology results from the BLM-induced lung damage study by Hafez et al. [46]. This may be clarified by the findings of Malaviya et al., who observed that macrophages that gathered in lung tissue shortly after lung toxicant damage were stimulated toward a pro-inflammatory M1 phenotype. This was demonstrated by morphologic changes, increased size and vacuolization, and lung TNF-α concentration a prototypical indicator of pro-inflammatory/cytotoxic macrophages [47]. As part of the host body's defense mechanism, inflammation is crucial because it helps the immune system identify and eliminate dangerous and foreign stimuli and start the healing process [48]. Uncontrolled inflammation can lead to long-term illnesses and tissue damage. TNF-α is the most significant pro-inflammatory cytokine that mediates the inflammatory response. TNF-α and other pro-inflammatory cytokines can further stimulate macrophages, causing them to release additional cytokines [49]. Furthermore, TNF-α stimulates edema and causes alveolar epithelial lung microvascular endothelial cells to undergo apoptosis [50]. Moreover, TNF-α levels in biopsy samples from pulmonary fibrosis patients were high [51]. This was consistent with the current study, which found a noteworthy elevation of TNF-α in the tissue homogenate of the GA3 group. The model group in the present study showed apparent collagen deposition surrounding airways, blood vessels, and in the interalveolar septa in addition to collapsing alveoli, as seen by Masson's trichrome stain. The morphometric data supported this since the model group's mean area % of collagen increased significantly in comparison to the negative control group. This is consistent with Bushra & Shenouda's findings that the GA3-treated rats had severe lung damage and excessive fibrosis as a result of reactive oxygen species (ROS) generation [52]. Shi et al.'s findings, which suggest that ROS might cause the deposition of collagen fibers and trigger profibrotic transforming growth factor-β activation, which increases fibroblast proliferation and leads to pulmonary fibrosis, may help to explain this [53]. According to the results of the present study, fibrosis started to show up around the end of the second week following GA3 injection. These results are consistent with those of Bassiouny et al., who after 14 days used bleomycin in an animal model of intrapulmonary fibrosis and obtained similar outcomes. According to their findings, bleomycin-induced chronic inflammation causes fibroblasts to become activated into myofibroblasts, which deposit collagen and secrete extracellular matrix [33].To evaluate the potential for disruption of the air-blood barrier due to collagen fiber deposition, the thickness of the inter-alveolar septum was examined. The current findings showed that, as compared to the negative control group, the lung sections of the GA3-treated rats had a much thicker interalveolar septum. This is consistent with earlier research findings that the morphometric study's considerable rise in the mean thickness of interalveolar septa was caused by an increase in collagen fibers and inflammatory cell infiltration into the septa [54]. Soliman et al.'s theory, according to which gibberellic acid attaches to ferrous molecules and DNA when it enters the target cell, may help to explain this. ROS are produced by this complex's oxidase-like action. These free oxygen radicals damage proteins and nucleic acids, boost the synthesis of collagen fibers, and induce lipid peroxidation, protein oxidation, and breakage in cellular DNA [4]. This process is what causes lung fibrosis to be induced in animal models [55,56].

One of the few reliable markers for identifying apoptotic cells is caspase-3. Following activation by different stimuli, the cell undergoes a series of signaling sequences that culminate in irreversible, controlled, and distinctive morphological changes before dying [57]. It has been discovered that GA3 increases apoptotic bodies in the hepatic parenchyma [34] and causes significant apoptosis in

spermatogenic cells [5,58]. According to recent research, the signaling cascade of caspase-3 activation can trigger pulmonary fibrosis through lung epithelial cell apoptosis [59]. Comparing GA3-treated animals to negative control animals, our immunohistochemical analysis revealed an intense cytoplasmic immune response for caspase-3 in the lining epithelial cells of bronchioles, alveoli, interalveolar septa, endothelial lining of some blood vessels, and along the exfoliated bronchial epithelial cells. The finding by Beigh et al. that inflammation causes apoptosis could help to explain this [60]. In humans and animals with acute lung injury, apoptosis has also been reported in type II alveolar, airway epithelial, and pulmonary endothelial cells [61].A key strategy for managing acute or chronic inflammatory illnesses is to reduce the generation of inflammatory mediators and inhibit the activity of inflammatory cells [17]. Omega-3 fatty acids and carotenoids abound in ChV, which also have anti-inflammatory and antioxidant qualities. Several investigations conducted in vitro and in vivo have reported on the anti-inflammatory properties of ChV extracts [62–65]. In both acute and long-term experimental inflammatory models, Swapnil Prakash Chaudhari et al. evaluated the anti-inflammatory efficacy of ChV. In this study, rats with carrageenan-induced paw edema had their extract's anti-inflammatory properties investigated at three distinct dosages (50 mg/kg, 100 mg/kg, and 200 mg/kg). In comparison to the control group, the treatment group's levels of cytokines (TNF-α, IL-6, and IL-1β) dropped [62]. In the current study, the increased TNF-α level was significantly reduced when ChV and GA3 were given together. According to Khadrawy et al. [24] and Farag et al. [66], our results were consistent. Additionally, Cheng et al. found that the mechanisms of *C. vulgaris's* defenses may be linked to its immunomodulatory action, which may boost natural killer cells and promote macrophages' phagocytic activity [67]. According to the results of the current study, *C. vulgaris* therapy is very effective when started at the beginning of GA3 treatment. Histopathologically, early ChV administration resulted in definite improvement of destructed lung tissue and even the restoration of normal alveolar architecture, which was confirmed by morphometric and statistical analysis, except for moderately thickened blood vessel wall, mildly thickened septa, and mild inflammatory cellular infiltration. According to these results, *C. vulgaris* significantly improved the lung tissue, and this improvement may have been brought about by early *C. vulgaris* therapy's direct ability to relieve lung fibrosis. Our results were supported by Zamri et al., who found that 300 mg/kg of ChV reduced the histological harm caused by cigarette smoke in the lungs. They discovered that when *C. vulgaris* was added to rats exposed to cigarette smoke, the lung tissue showed improvement in inflammation involving lymphocytes and plasma cells of the lungs [68].The present study's findings showed that, when compared to the GA3-treated group, there was a notable reduction in the area percentage of collagen fibers in the lung sections of the GA3/ChV-treated group. This is consistent with research by Mohseni et al., who examined *Chlorella vulgaris's* anti-fibrotic ability and linked it to its anti-apoptotic and anti-inflammatory characteristics [69]. Chlorella vulgaris was discovered to have a comparable protective effect against experimental airway inflammation in the guinea pig model [70]. Moreover, our findings demonstrated that giving rats ChV reduced the activation of caspase-3 in lung tissues. This outcome is consistent with the research conducted by Eissa et al., who discovered that Chlorella vulgaris exhibited anti-apoptotic activity and linked this behavior to its ability to inhibit caspase-3 [71].

4. Conclusion:

According to the current study's findings, GA3-intoxication causes the alveoli in the lung tissues to get smaller or even collapse, and this is accompanied by a high number of inflammatory cells. These histological and morphometric analyses point to lung fibrosis. In addition, there was a notable increase in apoptosis as shown by Caspase-3, and an increase in TNF-α. Nevertheless, the addition of ChV microalgae to the rats reversed all these aberrant alterations linked to GA3. Therefore, based on its anti-inflammatory and antiapoptotic properties, this study revealed that *C. vulgaris* is a prospective preventive drug against toxicity generated by GA3.

Acknowledgment:

The author thanks Ebtima Alofi for her support in writing some parts of this article, and thanks my departmental labs for helping in technical and experimental issues.

Conflicts of Interest:

The author declares that there is no conflicts of interest.

Funding:

The author did not get any financial support from any sponsors or labs.

5. References:

[1] W. El-Houseiny, A.H. Arisha, A. Behairy, M.M.M. Metwally, A.-W.A. Abdel-Warith, E.M. Younis, S.J. Davies, B.A. Hassan, Y.M. Abd-Elhakim, The immunosuppressive, growth-hindering, hepatotoxic, and oxidative stress and immune related-gene expressions-altering effects of gibberellic acid in Oreochromis niloticus: A mitigation trial using alpha-lipoic acid, Pestic. Biochem. Physiol. 198 (2024) 105725.

[2] A. Mukherjee, A.K. Gaurav, S. Singh, S. Yadav, S. Bhowmick, S. Abeysinghe, J.P. Verma, The bioactive potential of phytohormones: A review., Biotechnol. Reports (Amsterdam, Netherlands). 35 (2022) e00748. https://doi.org/10.1016/j.btre.2022.e00748.

[3] M.M.A. Hussein, H.A. Ali, M.M. Ahmed, Ameliorative effects of phycocyanin against gibberellic acid induced hepatotoxicity, Pestic. Biochem. Physiol. 119 (2015) 28–32.

[4] M.M. Soliman, A. Gaber, W.F. Alsanie, W.A. Mohamed, M.M.M. Metwally, A.A. Abdelhadi, M. Elbadawy, M. Shukry, Gibberellic acid-induced hepatorenal dysfunction and oxidative stress: mitigation by quercetin through modulation of antioxidant, anti-inflammatory, and antiapoptotic activities, J. Food Biochem. 46 (2022) e14069.

[5] R.A. Ahmed, A.E. Nofal, Ameliorating impact of Phoenix dactylifera L. leaves oil extract on testicular toxicity induced by gibberellic acid: histomorphometric and immunohistochemical studies, Egypt. J. Histol. 44 (2021) 128–143.

[6] X. Wang, W. Hao, Reproductive and developmental toxicity of plant growth regulators in humans and animals, Pestic. Biochem. Physiol. (2023) 105640.

[7] F. Farahat, N. Ibrahim, S. Elkhateeb, A. Shehata, Sub-Chronic Effects of Gibberellic Acid Repeated Exposure on the Testis of Adult Albino Rats (Biochemical, Histopathological and Immunohistochemical Study), Ain Shams J. Forensic Med. Clin. Toxicol. 20 (2013) 106–115.

[8] C.-S. Xu, Y. Zhou, Z. Jiang, L.-E. Wang, J.-J. Huang, T.-Y. Zhang, Y. Zhao, W. Shen, S.-H. Zou, L.-L. Zang, The in vitro effects of gibberellin on human sperm motility., Aging (Albany. NY). 11 (2019) 3080–3093. https://doi.org/10.18632/aging.101963.

[9] O.A. Abd-El-Aty, R.A. Masoud, Potential toxicity of plant growth regulator gibberellic acid (GA3) on the pancreatic structures and functions in the albino rat, Acad Anat Int. 2 (2016) 11–26.

[10] C.A. Damalas, I.G. Eleftherohorinos, Pesticide exposure, safety issues, and risk assessment indicators, Int. J. Environ. Res. Public Health. 8 (2011) 1402–1419.

[11] A. Troudi, A.M. Samet, N. Zeghal, Hepatotoxicity induced by gibberellic acid in adult rats and their progeny, Exp. Toxicol. Pathol. 62 (2010) 637–642.

[12] I. Celik, M. Turker, Y. Tuluce, Abcisic acid and gibberellic acid cause increased lipid peroxidation and fluctuated antioxidant defense systems of various tissues in rats, J. Hazard. Mater. 148 (2007) 623–629.

[13] N. Erin, B. Afacan, Y. Ersoy, F. Ercan, M.K. Balcı, Gibberellic acid, a plant growth regulator, increases mast cell recruitment and alters Substance P levels, Toxicology. 254 (2008) 75–81.

[14] J.-Y. Jeon, K.-E. Kim, H.-J. Im, S.-T. Oh, S.-U. Lim, H.-S. Kwon, B.-H. Moon, J.-M. Kim, B.-K. An, C.-W. Kang, The production of lutein-enriched eggs with dietary Chlorella, Food Sci. Anim. Resour. 32 (2012) 13–17.

[15] S. Buono, A.L. Langellotti, A. Martello, F. Rinna, V. Fogliano, Functional ingredients from microalgae, Food Funct. 5 (2014) 1669–1685.

[16] K. Rani, N. Sandal, P.K. Sahoo, A comprehensive review on chlorella-its composition, health benefits, market and regulatory scenario, Pharma Innov. J. 7 (2018) 584–589.

[17] H. Barghchi, Z. Dehnavi, E. Nattagh-Eshtivani, E.R. Alwaily, A.F. Almulla, A.K. Kareem, M. Barati, G. Ranjbar, A. Mohammadzadeh, P. Rahimi, N. Pahlavani, The effects of Chlorella vulgaris on cardiovascular risk factors: A comprehensive review on putative molecular mechanisms, Biomed. Pharmacother. 162 (2023) 114624. https://doi.org/https://doi.org/10.1016/j.biopha.2023.114624.

[18] L.M. Bauer, J.A.V. Costa, A.P.C. da Rosa, L.O. Santos, Growth stimulation and synthesis of lipids, pigments and antioxidants with magnetic fields in Chlorella kessleri cultivations, Bioresour. Technol. 244 (2017) 1425–1432.

[19] P.T. Bengwayan, J.C. Laygo, A.E. Pacio, J.L.Z. Poyaoan, J.F. Rebugio, A.L.L. Yuson, A comparative study on the antioxidant property of Chlorella (Chlorella sp.) tablet and glutathione tablet, E-International Sci. Res. J. 2 (2010) 25–35.

[20] M. Ebrahimi-Mameghani, Z. Sadeghi, M.A. Farhangi, E. Vaghef-Mehrabany, S. Aliashrafi, Glucose homeostasis, insulin resistance and inflammatory biomarkers in patients with non-alcoholic fatty liver disease: Beneficial effects of supplementation with microalgae Chlorella vulgaris: A double-blind placebo-controlled randomized clinical trial, Clin. Nutr. 36 (2017) 1001–1006.

[21] Y. Panahi, M.E. Ghamarchehreh, F. Beiraghdar, M. Zare, H.R. Jalalian, A. Sahebkar, Investigation of the effects of Chlorella vulgaris supplementation in patients with non-alcoholic fatty liver disease: a randomized clinical trial, Hepatogastroenterology. 59 (2012) 2099–2103.

[22] M. Sanayei, A. Izadi, F. Hajizadeh-Sharafabad, R. Amirsasan, M. Kaviani, A. Barzegar, Chlorella vulgaris in combination with high intensity interval training in overweight and obese women: a randomized double-blind clinical trial, J. Diabetes Metab. Disord. 20 (2021) 781–792.

[23] A.M. Hosseini, S.A. Keshavarz, E. Nasli-Esfahani, F. Amiri, L. Janani, The effects of Chlorella supplementation on glycemic control, lipid profile and anthropometric measures on patients with type 2 diabetes mellitus, Eur. J. Nutr. (2021) 1–11.

[24] S.M. Khadrawy, D.S. Mohamed, R.M. Hassan, M.A. Abdelgawad, M.M. Ghoneim, S. Alshehri, N.S. Shaban, Royal Jelly and Chlorella vulgaris Mitigate Gibberellic Acid-Induced Cytogenotoxicity and Hepatotoxicity in Rats via Modulation of the PPARα/AP-1 Signaling Pathway and Suppression of Oxidative Stress and Inflammation, Foods. 12 (2023) 1223.

[25] M.M. Soliman, A. Aldhahrani, A. Gaber, W.F. Alsanie, M. Shukry, W.A. Mohamed, M.M.M. Metwally, Impacts of n-acetyl cysteine on gibberellic acid-induced hepatorenal dysfunction through modulation of pro-inflammatory cytokines, antifibrotic and antioxidant activity, J. Food Biochem. 45 (2021) e13706.

[26] G.I. Aboul-Fotouh, M.B. Zickri, H.G. Metwally, I.R. Ibrahim, S.S. Kamar, W. Sakr, Therapeutic effect of adipose derived stem cells versus atorvastatin on amiodarone induced lung injury in male rat, Int. J. Stem Cells. 8 (2015)

170–180.
[27] J.D. Bancroft, C. Layton, Connective and mesenchymal tissues with their stains, Bancroft's Theory Pract. Histol. Tech. (2012) 187–214.
[28] R.A.B. Drury, E.A. Wallington, Preparation and fixation of tissues, Carleton's Histol. Tech. 5 (1980) 41–54.
[29] K.S. Suvarna, C. Layton, J.D. Bancroft, Bancroft's theory and practice of histological techniques E-Book, Immunohistochemical techniques, Bancroft's Theory Pract. Histol. Tech. (Eighth Ed. Elsevier. (2019) 337–94. https://doi.org/doi: 10.1016/B978-0-7020-6864- 5.00010-4.
[30] D.M. Zakaria, N.M. Zahran, S.A.A. Arafa, R.A. Mehanna, R.A. Abdel-Moneim, Histological and physiological studies of the effect of bone marrow-derived mesenchymal stem cells on bleomycin induced lung fibrosis in adult albino rats, Tissue Eng. Regen. Med. 18 (2021) 127–141.
[31] M.M. Soliman, A. Aldhahrani, A. Gaber, W.F. Alsanie, W.A. Mohamed, M.M.M. Metwally, M. Elbadawy, M. Shukry, Ameliorative impacts of chrysin against gibberellic acid-induced liver and kidney damage through the regulation of antioxidants, oxidative stress, inflammatory cytokines, and apoptosis biomarkers, Toxicol. Res. (Camb). 11 (2022) 235–244.
[32] S.-H. Dong, Y.-W. Liu, F. Wei, H.-Z. Tan, Z.-D. Han, Asiatic acid ameliorates pulmonary fibrosis induced by bleomycin (BLM) via suppressing pro-fibrotic and inflammatory signaling pathways, Biomed. Pharmacother. 89 (2017) 1297–1309.
[33] H.S. Bassiouny, A.S.E. Habib, A.M. Abdel Hameed, Histological Evaluation of The Possible Therapeutic Effect of Pirfenidone on Bleomycin-Induced Pulmonary Fibrosis in Adult Male Albino Rats, Egypt. J. Histol. 46 (2023) 19–32.
[34] A.E. Alsemeh, R.S. Moawad, E.R. Abdelfattah, Histological and biochemical changes induced by gibberellic acid in the livers of pregnant albino rats and their offspring: ameliorative effect of Nigella sativa, Anat. Sci. Int. 94 (2019) 307–323.
[35] O. Desai, J. Winkler, M. Minasyan, E.L. Herzog, The role of immune and inflammatory cells in idiopathic pulmonary fibrosis, Front. Med. 5 (2018) 43.
[36] W. Ornatowski, Q. Lu, M. Yegambaram, A.E. Garcia, E.A. Zemskov, E. Maltepe, J.R. Fineman, T. Wang, S.M. Black, Complex interplay between autophagy and oxidative stress in the development of pulmonary disease, Redox Biol. 36 (2020) 101679.
[37] S. Han, R.K. Mallampalli, The Role of Surfactant in Lung Disease and Host Defense against Pulmonary Infections., Ann. Am. Thorac. Soc. 12 (2015) 765–774. https://doi.org/10.1513/AnnalsATS.201411-507FR.
[38] J.A. Whitsett, S.E. Wert, T.E. Weaver, Alveolar surfactant homeostasis and the pathogenesis of pulmonary disease., Annu. Rev. Med. 61 (2010) 105–119. https://doi.org/10.1146/annurev.med.60.041807.123500.
[39] C. Keskinidou, A.G. Vassiliou, I. Dimopoulou, A. Kotanidou, S.E. Orfanos, Mechanistic Understanding of Lung Inflammation: Recent Advances and Emerging Techniques., J. Inflamm. Res. 15 (2022) 3501–3546. https://doi.org/10.2147/JIR.S282695.
[40] L. Knudsen, E. Lopez-Rodriguez, L. Berndt, L. Steffen, C. Ruppert, J.H.T. Bates, M. Ochs, B.J. Smith, Alveolar Micromechanics in Bleomycin-induced Lung Injury., Am. J. Respir. Cell Mol. Biol. 59 (2018) 757–769. https://doi.org/10.1165/rcmb.2018-0044OC.
[41] E. El Bana, L. Shawky, The appropriate time for stem cell transplantation in albino rat with amiodarone induced lung fibrosis: histological and immunohistochemical study, Egypt. J. Histol. 42 (2019) 121–132.
[42] M.F. Abdel-Rahman, D.B. El-Azhari, H.M. Amin, The potential protective role of vitamins C against adverse effects of some plant growth regulators in albino rats, J. Pharm. Negat. Results. (2023) 337–346.
[43] A.F. Ali, N.S. Ghoneim, R. Salama, Light and electron microscopic study on the effect of Gibberellic acid on the renal cortex of adult male albino rats and the possible protective role of coenzyme Q10, Egypt. J. Histol. 44 (2021) 368–383.
[44] M.-R. Ghigna, P. Dorfmüller, Pulmonary vascular disease and pulmonary hypertension, Diagnostic Histopathol. 25 (2019) 304–312.
[45] M.Y. Kamel, S.M. Ahmed, W.Y. Abdelzaher, N.N. Welson, A.M. Abdel-Aziz, Role of IL-6/STAT3 pathway in mediating the protective effect of agomelatine against methotrexate-induced lung/intestinal tissues damage in rats, Immunopharmacol. Immunotoxicol. 44 (2022) 35–46.
[46] S.M.N.A. Hafez, E.A. Saber, N.M. Aziz, M.Y. Kamel, A.A. Aly, E.-S.M.N. Abdelhafez, M.F.G. Ibrahim, Potential protective effect of 3,3'-methylenebis(1-ethyl-4-hydroxyquinolin-2(1H)-one) against bleomycin-induced lung injury in male albino rat via modulation of Nrf2 pathway: biochemical, histological, and immunohistochemical study., Naunyn. Schmiedebergs. Arch. Pharmacol. 396 (2023) 771–788. https://doi.org/10.1007/s00210-022-02324-1.
[47] R. Malaviya, J.D. Laskin, D.L. Laskin, Anti-TNFα therapy in inflammatory lung diseases, Pharmacol. Ther. 180 (2017) 90–98.
[48] P. Bansal, D. Verma, S. Singh Tamber, R. Sharma, An update on pathogenesis of inflammatory disorders with its management, RPS Pharm. Pharmacol. Reports. 2 (2023) rqad011.
[49] J.K. Sethi, G.S. Hotamisligil, Metabolic messengers: tumour necrosis factor, Nat. Metab. 3 (2021) 1302–1312.
[50] H.-L. Lu, X.-Y. Huang, Y.-F. Luo, W.-P. Tan, P.-F. Chen, Y.-B. Guo, Activation of M1 macrophages plays a critical role in the initiation of acute lung injury, Biosci. Rep. 38 (2018) BSR20171555.
[51] E.H. Alhamad, J.G. Cal, Z. Shakoor, A. Almogren, A.A. AlBoukai, Cytokine gene polymorphisms and serum cytokine levels in patients with idiopathic pulmonary fibrosis, BMC Med. Genet. 14 (2013) 1–13.
[52] R.R. Bushra, M.B. Shenouda, The possible protective role of N-acetylcysteine against gibberellic acid-induced lung structural changes of the adult albino rat, Egypt. J. Histol. 46 (2023) 603–618.
[53] K. Shi, J. Jiang, T. Ma, J. Xie, L. Duan, R. Chen, P. Song, Z. Yu, C. Liu, Q. Zhu, Pathogenesis pathways of idiopathic pulmonary fibrosis in bleomycin-induced lung injury model in mice, Respir. Physiol. Neurobiol. 190 (2014) 113–117.
[54] M.Y. Salem, N.E.-E. El-Azab, E.M. Faruk, Modulatory effects of green tea and aloe vera extracts on experimentally-induced lung fibrosis in rats: histological and immunohistochemical study, J. Histol. Histopathol. 1 (2014) 6.

[55] B. B. Moore, W.E. Lawson, T.D. Oury, T.H. Sisson, K. Raghavendran, C.M. Hogaboam, Animal models of fibrotic lung disease, Am. J. Respir. Cell Mol. Biol. 49 (2013) 167–179.
[56] I.A. Savin, M.A. Zenkova, A. V Sen'kova, Pulmonary fibrosis as a result of acute lung inflammation: molecular mechanisms, relevant in vivo models, prognostic and therapeutic approaches, Int. J. Mol. Sci. 23 (2022) 14959.
[57] D.R. McIlwain, T. Berger, T.W. Mak, Caspase functions in cell death and disease, Cold Spring Harb. Perspect. Biol. 5 (2013) a008656.
[58] E.M. El-Beltagi, W.M. Elwan, N.A.M. El-Bakry, E.F. Salah, Histological and immunohistochemical study on the effect of gibberellic acid on the seminiferous tubules of testis of adult albino rat and the possible protective role of grape seeds proanthocyanidin extract, Tanta Med. J. 45 (2017) 79.
[59] J.-M. Lee, M. Yoshida, M.-S. Kim, J.-H. Lee, A.-R. Baek, A.S. Jang, D.J. Kim, S. Minagawa, S.S. Chin, C.-S. Park, Involvement of alveolar epithelial cell necroptosis in idiopathic pulmonary fibrosis pathogenesis, Am. J. Respir. Cell Mol. Biol. 59 (2018) 215–224.
[60] S. Beigh, H. Rashid, S. Sharma, S. Parvez, S. Raisuddin, Bleomycin-induced pulmonary toxicopathological changes in rats and its prevention by walnut extract, Biomed. Pharmacother. 94 (2017) 418–429.
[61] T.R. Martin, N. Hagimoto, M. Nakamura, G. Matute-Bello, Apoptosis and epithelial injury in the lungs, Proc. Am. Thorac. Soc. 2 (2005) 214–220.
[62] S.P. Chaudhari, D.T. Baviskar, Anti-inflammatory Activity of Chlorella vulgaris in Experimental models of Rats., Int. J. Pharm. Investig. 11 (2021).
[63] G. Sibi, S. Rabina, Inhibition of pro-inflammatory mediators and cytokines by Chlorella vulgaris extracts, Pharmacognosy Res. 8 (2016) 118.
[64] J.H. Kwak, S.H. Baek, Y. Woo, J.K. Han, B.G. Kim, O.Y. Kim, J.H. Lee, Beneficial immunostimulatory effect of short-term Chlorella supplementation: enhancement of natural killer cell activity and early inflammatory response (randomized, double-blinded, placebo-controlled trial), Nutr. J. 11 (2012) 1–8.
[65] W. Soontomchaiboon, S.S. Joo, S.M. Kim, Anti-inflammatory effects of violaxanthin isolated from microalga Chlorella ellipsoidea in RAW 264.7 macrophages, Biol. Pharm. Bull. 35 (2012) 1137–1144.
[66] M.R. Farag, M. Alagawany, E.A.A. Mahdy, E. El-Hady, S.M. Abou-Zeid, S.A. Mawed, M.M. Azzam, G. Crescenzo, A.M.A. Abo-Elmaaty, Benefits of Chlorella vulgaris against Cadmium Chloride-Induced Hepatic and Renal Toxicities via Restoring the Cellular Redox Homeostasis and Modulating Nrf2 and NF-KB Pathways in Male Rats., Biomedicines. 11 (2023). https://doi.org/10.3390/biomedicines11092414.
[67] D. Cheng, Z. Wan, X. Zhang, J. Li, H. Li, C. Wang, Dietary Chlorella vulgaris ameliorates altered immunomodulatory functions in cyclophosphamide-induced immunosuppressive mice, Nutrients. 9 (2017) 708.
[68] K.S. Zamri, M.K.N. Norripin, F.I. Darus, D.G. Ekambaram, N.D. Abdul Raof, N.H. Roslan, Y.A. Mohd Yusof, Protective effect of Chlorella vulgaris on dna damage, oxidative stress, and lung morphological changes in cigarette smoke-exposed rats, Asian J. Pharm. Clin. Res. 11 (2018) 145–149.
[69] R. Mohseni, S.M. Alavian, Z.A. Sadeghabadi, M. Heiat, Therapeutic effects of Chlorella vulgaris on carbon tetrachloride induced liver fibrosis by targeting Hippo signaling pathway and AMPK/FOXO1 axis, Mol. Biol. Rep. 48 (2021) 117–126.
[70] P. Capek, M. Matulová, M. Šutovská, J. Barboríková, M. Molitorisová, I. Kazimierová, Chlorella vulgaris α-L-arabino-α-L-rhamno-α, β-D-galactan structure and mechanisms of its anti-inflammatory and anti-remodelling effects, Int. J. Biol. Macromol. 162 (2020) 188–198.
[71] M.M. Eissa, M.M. Ahmed, M.A. Abd Eldaim, A.A. Mousa, A.F. Elkirdasy, M.A. Mohamed, S.H. Orabi, Chlorella vulgaris ameliorates sodium nitrite-induced hepatotoxicity in rats, Environ. Sci. Pollut. Res. 28 (2021) 9731–9741.